

## Research Article

## A Numerical Study on the Effect of Urea Formaldehyde Microcapsules Filling Ratio on the Deformation of Epoxy Composites using Finite Element Method (FEM)

E. Katouezadeh<sup>1</sup>, M. Ebadi<sup>2</sup>, S.M. Zebarjad<sup>1\*</sup> and K. Janghorban<sup>1</sup><sup>1</sup> Department of Materials Science and Engineering, Engineering Faculty, Shiraz University, Shiraz, Iran<sup>2</sup> Department of Civil Engineering, Marvdasht Branch, Islamic Azad University, Marvdasht, Iran

## ARTICLE INFO

*Article history:*

Received 6 February 2022

Reviewed 8 March 2022

Revised 30 March 2022

Accepted 9 April 2022

*Keywords:*

Microcapsule  
Composite  
Epoxy  
Urea formaldehyde  
Finite element method

## ABSTRACT

In recent years, many new material configurations have emerged from which hybrid materials such as microcomposites have shown promising applications. In the current study, the microencapsulated-based epoxy composites were simulated in micro and macro-scales using numerical modeling. A single-microcapsule was simulated by finite element method (FEM) to estimate the effect of compression on a representative equivalent volume (REV). FEM sensitivity analysis was conducted for different conditions of encapsulation efficiency, i.e., full, half-full and empty, varied diameter (50, 100, 200  $\mu\text{m}$ ) and thickness (2, 6, 10  $\mu\text{m}$ ) of capsules to study the influence of each governing parameter on the load-deformation behavior of the composite. The composites containing microcapsules with full content showed an improvement in the elastic modulus in comparison with the neat epoxy, while half-full and empty composites exhibited lower elastic moduli. Moreover, the results showed that the diameter of the capsules significantly influences the stiffness of the composite. Indeed, the overall elastic modulus of the 50  $\mu\text{m}$  microcapsules was slightly affected by the encapsulation efficiency while the 200  $\mu\text{m}$  microcapsules showed a drop of 28% in their elastic modulus from the full to the empty capsule condition. Finally, the load-deformation behavior of the composite was studied in macro-scale based on the elastic moduli calculated from micro-scale modeling of an REV.

© Shiraz University, Shiraz, Iran, 2022

### 1. Introduction

Recently, self-healing smart material developments have been under extensive attention as an cutting-edge approach [1, 2]. They are defined as the materials that can heal damages automatically to restore the functionality of materials. The ability to self-heal would result in prolonged material service life, less maintenance, and therefore cost reductions. This phenomenon was conceived by biomimetics or

biologically inspired technologies by nature [3]. The potential benefits of self-healing materials have provided the motivation for a major research effort on self-healing materials, which has been reported in an ever-expanding body of literature [4-7]. These materials have ranged from polymer matrix composites to ceramic matrix composites or even metals [8]. Microcapsules that are incorporated in the polymer composite material contain the self-healing agents that can polymerize or crosslink upon rupture of the capsules as a result of

\* Corresponding author

E-mail address: [mojtabazebarjad@shirazu.ac.ir](mailto:mojtabazebarjad@shirazu.ac.ir) (S.M. Zebarjad)<https://doi.org/10.22099/IJMF.2022.42996.1216>

mechanical damage [9, 10]. In fact, the encapsulated self-healing agent is self-triggered or externally triggered after the crack occurrence at the surface. Although, the autonomous systems may have many advantages, some difficulties limit their applicability. Using oxidative healing agents, which do not require any catalyst, can solve this problem. In the following, unsaturated drying oils as the core materials showed the self-healing ability without any catalyst [11]. Selection of the most suitable encapsulation method depends on the type of core and shell, application and size of microcapsules, physical and chemical properties of core and shell, release mechanism, production scale and cost [12].

Barbero and Ford [13] conducted experimental studies in the field of continuum damage mechanics and investigated damage and self-healing by capsules. Rue et al. [14] discussed the volume of the healing agent that reaches the crack and concluded that it is linearly dependent on the microcapsule size as well as volume fraction. Zhang et al. [15] reviewed many analytical studies developed for the self-healing polymers based on different approaches. Moreover, as the spherical capsules can release the healing agent from a limited distance to the crack, other stretched shapes were analyzed to investigate the efficiency of the self-healing composites [16]. In addition, Mookheok [17] extended the concept of elongated capsules and illustrated that the efficiency of healing can be doubled when the length of the capsules is increased. A simplified case in which an infinite crack hits a number of capsules in the matrix of a self-healing composite has been investigated by many researchers [18, 19]. On the other hand, analysis of the healing-efficiency of a limited size crack that randomly occurred in the matrix of a self-healing composite is still an open issue [20]. Moreover, Zemskov [21] analyzed the healing probability in a very simplified two dimensional model using elementary formulas of probability.

To the best of our knowledge, despite the expanded experimental research conducted in investigating the effect of different parameters and mechanisms of self-healing behavior and limiting the domain of knowledge to the experimental studies restricts the applicability of these materials. Additionally, making and testing these

materials is costly and time and energy consuming. To overcome this problem, numerical methods such as finite element method (FEM) and finite difference method (FDM) have been widely used [22, 23]. In fact, there are a limited number of studies which proposed analytical and numerical modeling on the characterization of encapsulation-based self-healing composites. Hence, it is believed that the numerical study on the mechanical behaviors of the microcapsules-based composites can be considered as a major literature gap which is going to be extensively used in self-healing materials. In this regard, the authors investigated the mechanical properties of epoxy composites containing oil-filled microcapsules and indicated their softening effect [24]. The effect of the capsule size and shell thickness on the mechanical behavior of microencapsulated-based composites is still unclear. The numerical modeling, performed in micro and macro scale, helped discover the limitations of the experimental studies while the flexibility of the geometry and input parameters for the models helped analyze and interpret a wide range of conditions that were too hard or impossible to investigate experimentally.

In the current study, potential conditions and major governing parameters on the mechanical behavior of the microencapsulated-based epoxy composites were simulated and analyzed in micro and macro-scales using numerical modeling. At different conditions of encapsulation efficiency (i.e., full, half-full and empty), a single-microcapsule was simulated by 2D finite element method (FEM) to estimate the effect of compression on a representative equivalent volume (REV). FEM sensitivity analysis was conducted for different conditions of encapsulation efficiency, varied diameter and thickness of capsules to study the load-deformation behavior of the composite in these potential conditions. Lastly, the load-deformation behavior of the composite was simulated in macro-scale using the elastic moduli calculated from micro-scale modeling of an REV.

## **2. Modeling**

The modeling studies are devoted to the input parameters required for the simulation. For this reason,

results of research studies conducted by Katouezadeh et al. [19, 25, 26] on the self-healing materials were analyzed. Urea formaldehyde (UF) microcapsules containing linseed oil were prepared by in situ polymerization and optimized by the design of experiments (DOE) methods [25]. The following approach is generally based on the outcome of experimental results directly taken into account and is simplified to be comprehensible for practical applications.

### 2.1. Analytical modeling

A schematic representation of a microcapsule and its elements has been illustrated in Fig. 1, and Eq. (1). It is undeniable that accepting a totally uniform distribution of the capsules with identical diameters is idealistic but this simplification can provide a better understanding about the composite, its components and the parameters that govern the total number of microcapsules, their average diameter and shell thickness. As shown in Fig. 1, a typical microcapsule is consisted of a core from a healing agent, covered by a shell in a round shape. On the other hand, the average diameter of the microcapsules can be engineered and determined by following appropriate mechanisms of production [27, 28].

According to Eq. (2), the average mass of the capsule can be derived based on the density and volume of each element (i.e., shell and core), assuming a volumetric average diameter for the capsules. Hence, the total mass of the capsules would be "n" times of the single capsule mass, which gives the number of the capsules, "n", Eq. (3). Therefore, the average spacing of the microcapsules can be estimated as Eq. (4).

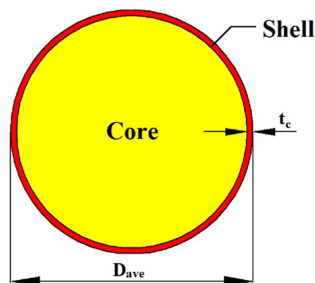


Fig. 1. Schematic illustration of a capsule including shell and core elements.

$$D_{core} = D_{ave} - 2t_c \quad (1)$$

$$\begin{aligned} m_{ave\_caps} &= \rho_{core} \left( \frac{\pi}{6} (D_{core})^3 \right) \\ &+ \rho_{shell} \left( \frac{\pi}{6} (D_{ave}^3 - D_{core}^3) \right) \\ &= \frac{\pi}{6} [\rho_{core} (D_{ave} - 2t_c)^3 \\ &+ \rho_{shell} ((D_{ave}^3 - (D_{ave} - 2t_c)^3)] \end{aligned} \quad (2)$$

$$n = \frac{m_{t\_caps}}{m_{ave\_caps}} \quad (3)$$

$$V_t = n \cdot S^3 \rightarrow S = \sqrt[3]{\frac{V_{t\_mat}}{n}} \quad (4)$$

$m_{ave\_caps}$ : Average mass of each capsule

$t_c$ : Thickness of the shell of the capsules

$\rho_{shell}$ : Density of the shell material

$\rho_{core}$ : Density of the core material

$D_{ave}$ : Average diameter of the capsules

$D_{core}$ : Diameter of the core

$m_{t\_caps}$ : Total mass of the capsule

$V_{t\_mat}$ : Total volume of the matrix

Accepting an average spacing between the microcapsules gives a uniform average arrangement in which a capsule is located at the center of an equivalent cubic cell of dimension S, as shown in Fig. 2.

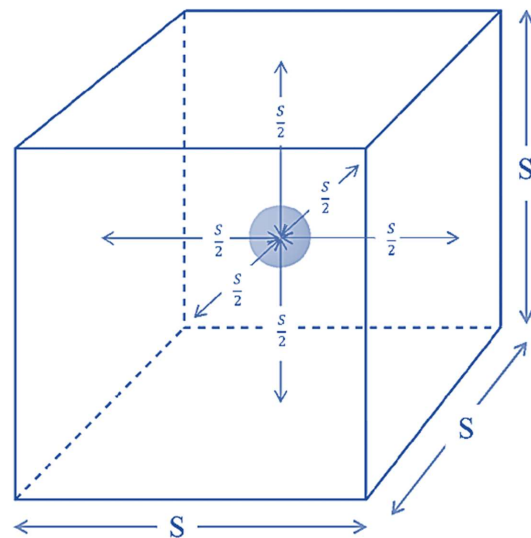


Fig. 2. A single microcapsule at the center of an equivalent cubic cell of dimension S.

The healing process mainly depends on the volume of the encapsulated healing agent. In addition, the number of capsules multiplies the effect of an individual, and therefore, healing depends on both the volume of the capsules and their number. On the other hand, the capsules do not have a uniform size distribution and an inhomogeneous dispersion in the matrix, which makes it impractical to obtain an average spacing between the capsules and evaluate the healing efficiency. Therefore, an average diameter, as well as an average spacing, is assumed to provide a simple, comprehensible, and practical evaluation of the encapsulated polymer composite and its healing efficiency for different conditions [19].

## 2.2. Numerical modeling

The schematic volume illustrated in Fig. 2 can be considered as the basis of introducing a representative equivalent volume (REV) to further investigate the composite on a micro-scale using finite element method (FEM).

Prior to commencing the specific modeling for the current study, and in order to verify the accuracy of the simulations, a simple model including a single point load on an elastic material was analyzed and the results were compared to the available closed-form solution for this problem. The results showed a less than 0.5% difference which verifies the accuracy of the modeling.

As multiplication of the REV produces the composite in macro-scale, the boundary conditions should also be defined correctly. In this regard, the upper surface of the REV is only subjected to the prescribed displacement and does not have any supports. On the other hand, side surfaces of the REV have roller supports which give them freedom for vertical displacement but limits lateral horizontal displacement which is in compliance with the confinement of the REV by the surrounding material in the composite. Lastly, the bottom of the REV has fixed support to bring vertical force equilibrium and horizontal confinement.

The material properties used for modeling the epoxy composite are tabulated in Table 1 and are selected based on the experimental results from the literature [29, 30].

Elastic material model was applied to the model due to its simplicity and coverage of the goals of this study. Oil as the core of microcapsules was supposed to be an extremely weak material with very low elastic modulus of 0.001 MPa to simplify the fluid phase while Poisson's ratio of about 0.5 guarantees the incompressible behavior of the oil [31].

**Table 1.** Material properties used for FEM modeling [29, 30]

Material	$\gamma$ (kN/m <sup>3</sup> )	E (MPa)	$\nu$
Neat Epoxy	11	3350	0.32
UF (Shell)	12	800	0.3
Drying Oil* (Core)	9.3	0.001	0.5

\* Linseed oil properties were selected for this study.

In order to model the micro-scale REV, a 2D axis-symmetric model was analyzed based on the material properties presented in Table 1 and in compliance with the geometry previously shown in Fig. 2. Specifications of the numerical models are as presented in Table 2.

**Table 2.** Specifications of the numerical models

Item	Details
Analysis Methods	FEM
Mesh Type	15 noded Triangular Graded Mesh
Model Geometry	Axi-symmetric

The diameter of the capsules (D), their spacing (S) and the thickness of the shell (t) were considered as the major micro-scale geometrical specifications of the capsules to conduct a sensitivity analysis to investigate the influence of variations of each parameter on the mechanical properties of the composite. Ranges of variation and values of the geometrical parameters in FEM models are shown in Table 3. According to the studies conducted on self-healing microcapsules-based composites, the size of microcapsules plays an important role in the healing efficiency [32]. Although the bigger capsules will contain more healing agents and correspondingly the crack incidence probability is higher, but the mechanical strength of the composite would drastically decrease [32]. Hence, the optimum size of the capsules was considered to be less than 200  $\mu\text{m}$  [33-36]. Meanwhile, as different diameters (50, 100, 200  $\mu\text{m}$ ) with varied thicknesses (2, 6, 10  $\mu\text{m}$ ) are being considered for this investigation, the selected spacing

gives different D/S values which are reasonable for this study. Moreover, it should be mentioned that the content of microcapsules, known as encapsulation efficiency, is not always fully perfect [37, 38]. It can be caused due to their production method, as well as the manufacturing technique which may diminish the microcapsules yield over time. Accordingly, the encapsulation efficiency is defined in three stages, i.e., full, half-full and empty.

**Table 3.** Range of parameter variations in sensitivity analysis

Item	Range
D ( $\mu\text{m}$ )	50
	100
	200
t ( $\mu\text{m}$ )	2
	6
	10
Encapsulation Efficiency	Full, Half-Full, Empty

In order to evaluate the load-deformation behavior of the neat epoxy and composite the compressive behavior of the composite was simulated in macro-scale. An illustrative cylindrical sample has been modeled with the dimension of 12.7 mm in diameter and 25.4 mm in height to evaluate the stress distribution pattern and uniformity in the bulk material. Similar to micro-scale studies, FEM was used for numerical modeling. Regarding the cylindrical shape of the sample, axisymmetric modeling was selected.

It should be noted and emphasized that while the generalization of the REV (in micro-scale) to the macro-scale behavior does not bring ultimate accuracy, it is an efficient method to investigate different cases and obtain illustrative results that show the trend of composite material behavior.

### 3. Results and Discussion

Figs. 3(a) to 3(c) show that the FEM model and its mesh distribution for the 50  $\mu\text{m}$ , 100  $\mu\text{m}$ , and 200  $\mu\text{m}$  diameters, respectively. The REV is subjected to a uniform load on top and its boundaries are defined to be free for vertical deformation and fixed for lateral deformation. It should be noted that the shells of the capsules are modeled using the plate element [39].

Triangular graded FEM mesh is selected for this model and the mesh size is finer near the capsules to obtain higher accuracies in this zone [40].

This sensitivity analysis was initiated with the stress and displacement distribution studies in the REV. Fig. 4 shows illustrative vertical stress distribution in the REV for full, half-full and empty microcapsules. In this regard, Figs. 4(a) to 4(c) show the vertical stress distribution in the REV for 2  $\mu\text{m}$  shell thickness in full, half-full and empty microcapsule conditions for 50  $\mu\text{m}$ , 100  $\mu\text{m}$  and 200  $\mu\text{m}$  diameters, respectively. The results in general show that the trend of stress distribution is almost the same for all conditions. Meanwhile, for full microcapsules with higher diameters, the inner capsule stress (i.e., oil pressure) highly amplifies. Moreover, for the half-full condition, the oil pressure dramatically falls. Furthermore, the stress distribution in the REV for empty microcapsules shows much lower maximum stress in the matrix which can be interpreted as a result of omitting the incompressible element (i.e., oil) from the load bearing elements. It should be also added that the stress distribution of the oil (in the microcapsules) presented in the shapes is not realistic because the liquid

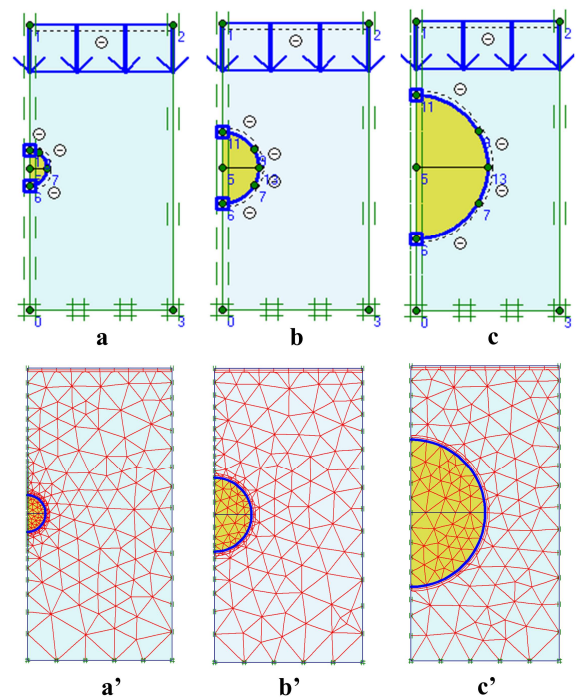


**Fig. 3.** FEM model and its mesh distribution for the REV: (a, a') 50  $\mu\text{m}$ , (b, b') 100  $\mu\text{m}$  and (c, c') 200  $\mu\text{m}$  diameters.

oil shows hydrostatic pressure distribution in half-full condition and an almost uniform pressure distribution in full capsule conditions.

Additionally, Fig. 5 shows illustrative vertical displacement results in the REV. More specifically, Figs. 5(a) to 5(c) show the vertical displacement distribution

in the REV obtained for 2  $\mu\text{m}$  shell thickness in full, half-full and empty microcapsule conditions for 50  $\mu\text{m}$ , 100  $\mu\text{m}$  and 200  $\mu\text{m}$  diameters, respectively. Like the stress distribution in the REV, vertical displacement in the REV follows a general pattern which can be seen for all conditions. Meanwhile, for larger diameters the influence

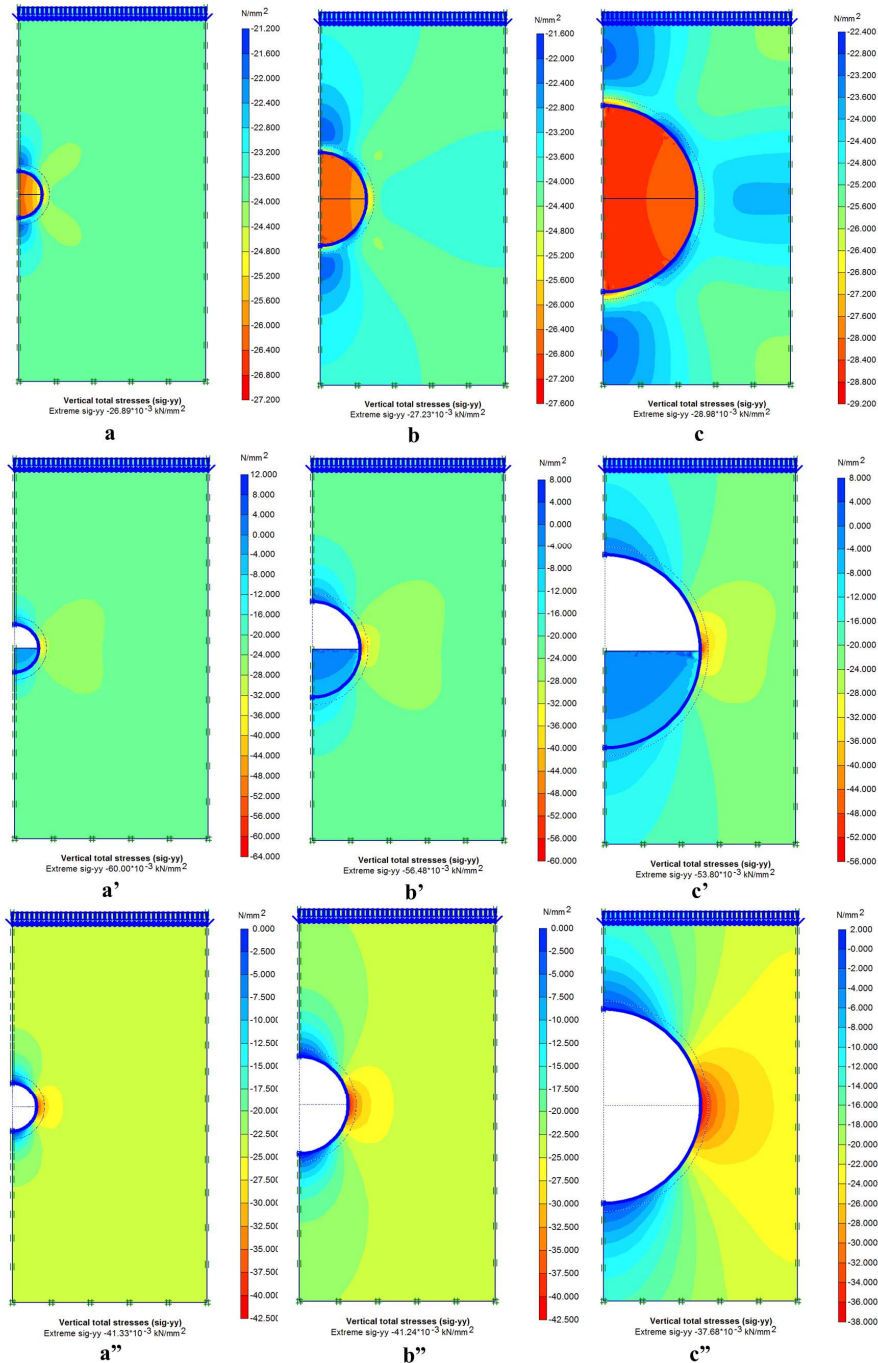


Fig. 4. Vertical stress distribution in the REV for full, half-full and empty microcapsule conditions: (a, a', a'') 50  $\mu\text{m}$ , (b, b', b'') 100  $\mu\text{m}$  and (c, c', c'') 200  $\mu\text{m}$  diameters with 2  $\mu\text{m}$  shell thickness.

of the microcapsules becomes more significant. In specific, as the emptiness of the capsule increases, the vertical displacement around it and mostly on top of it increases accordingly, which is much more recognizable for higher microcapsule diameters. It should be added

that the results for the displacement distribution in the oil for half-full condition is not dependable due to the non-modeled nature of the liquid phase that causes flow under deformations.

Presence of microcapsules in the REV changed the

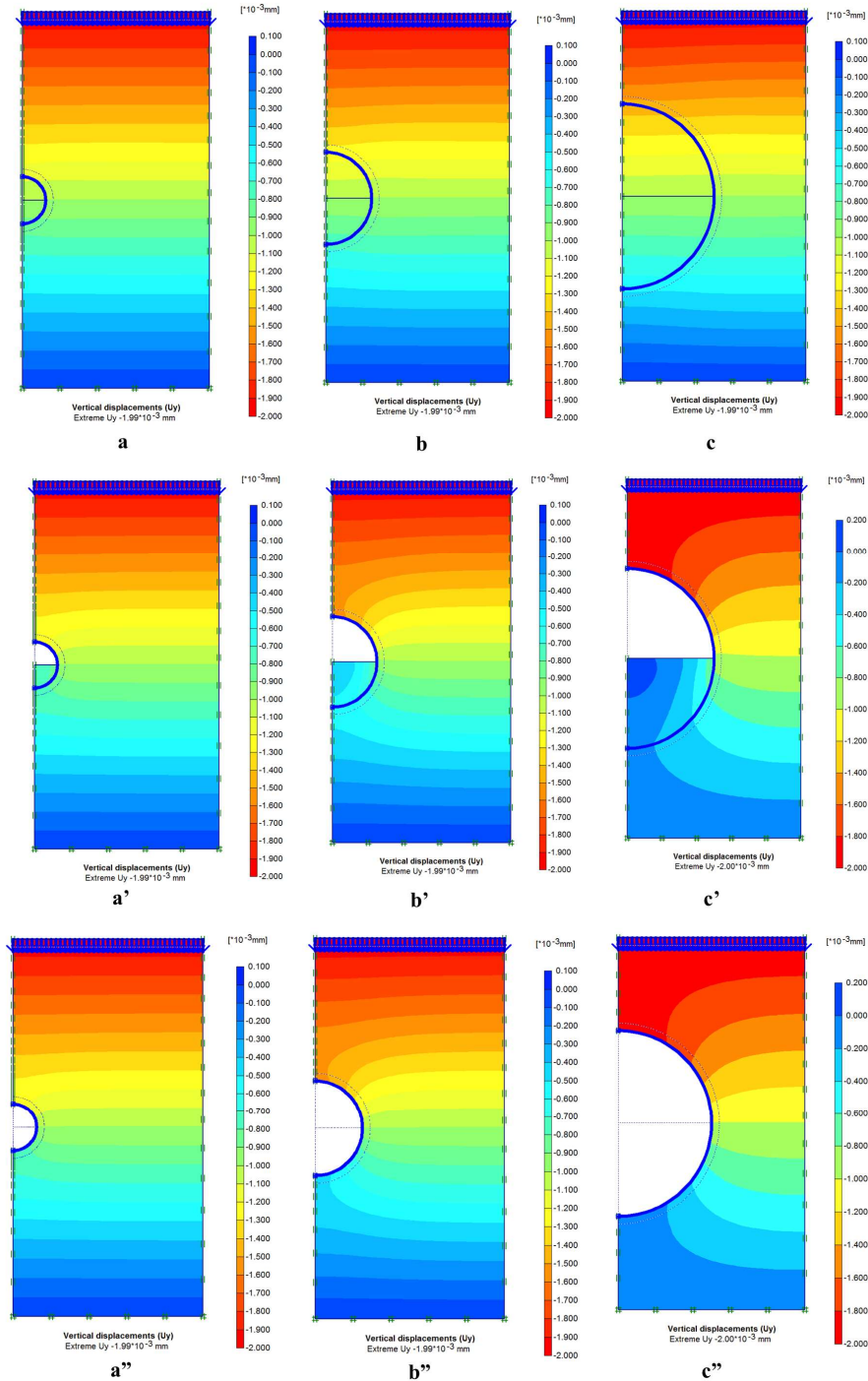


Fig. 5. Vertical displacement distribution in the REV for full, half-full and empty microcapsule conditions: (a, a', a'') 50  $\mu\text{m}$ , (b, b', b'') 100  $\mu\text{m}$  and (c, c', c'') 200  $\mu\text{m}$  diameters with 2  $\mu\text{m}$  shell thickness.

overall elastic modulus which was investigated for all different conditions. In this regard, the stress on the top of the REV due to the 0.005 strain was extracted from the outputs. The results showed that in general, for small microcapsules, the stress distribution is almost rectangular while for the large microcapsule, this distribution is rather trapezoid with lower stress on the sides and higher above the microcapsules. By dividing the average stress on top of the REV due to the imposed stress, the constrained elastic modulus was determined. The constrained condition is the result of horizontal fixities in the lateral exteriors of the REV. The general elastic modulus can be derived from the constrained elastic modulus by following basics of solid mechanics [41], as presented in Eq. (5).

$$E = E_{constrained} \frac{(1 - 2\vartheta)(1 + \vartheta)}{(1 - \vartheta)} \quad (5)$$

Fig. 6 shows the elastic moduli under different conditions including different sizes of the capsules, shell thickness and encapsulation efficiency. The results show the elastic modulus of the full capsule case with diameters of 100 and 200 μm, is higher than the neat epoxy (3.35 GPa). It can be inferred as a result of non-compressible oil in the microcapsules which reduces their vertical displacement and increases the vertical stress around the microcapsules. Moreover, it can be seen that this effect is much more significant for the 200 μm microcapsules (3.43 GPa). This is because larger microcapsules occupy higher volume portions of the REV in comparison with the smaller microcapsules.

Furthermore, it can be seen that the influence of encapsulation efficiency on the elastic moduli is much more significant for the larger capsules. Indeed, for 50 μm microcapsules, the effect of core content on the results is almost negligible while for the 200 μm microcapsules, the elastic modulus drops more than 28% for the empty condition in comparison with the full condition. In addition, it can be seen that the difference between full and half-full condition is considerable (i.e., plummet from 3.43 to 2.51 GPa), while small differences can be identified between the half-full and empty microcapsule conditions. While the experimental results

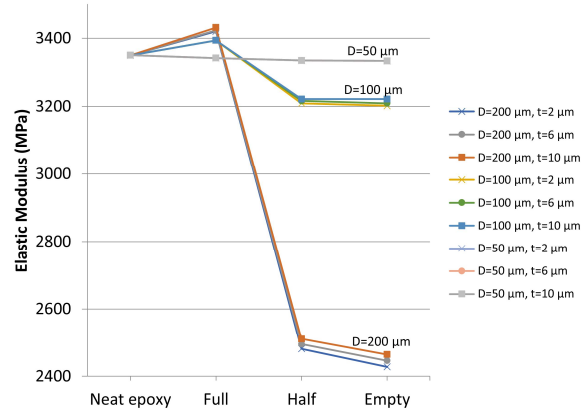


Fig. 6. Elastic moduli variation for different modeled conditions.

from the literature [24, 42], show a decrease in the elastic modulus of encapsulated composites, the drop in the elastic modulus for half-full and empty conditions (Fig. 6) demonstrates that the majority of the microcapsules in the reported experimental results from the literature are not full. This issue has been considered and reported as the encapsulation efficiency or microcapsules yield which is measured by thermal analysis or extraction methods [38, 43]. Additionally, it is clear that the shell thickness has little influence on the results while in general, higher thicknesses provide higher elastic moduli due to the increased strength of the microcapsules.

The axial force in the shell was also investigated. As shown in Fig. 7, the axial force in the capsules is directly dependent on the emptiness of the microcapsules, diameter of the microcapsules, and much more importantly, the shell thickness. Specifically, the most important parameter is shell thickness which shows an increase from 30 to 70 mN at a diameter of 100 μm, and generally the highest axial force results from the empty microcapsule conditions. This effect becomes much more recognizable for higher shell thicknesses at full, half-full and empty conditions. In addition, the emptiness of the microcapsules generally increases the axial force in the shell. Clearly, for the full microcapsule condition, the incompressibility of the inner oil provides support for the shell which leads to a decrease in the axial force in the shell. Furthermore, it can be seen that for higher microcapsule diameters, the axial force is slightly higher.

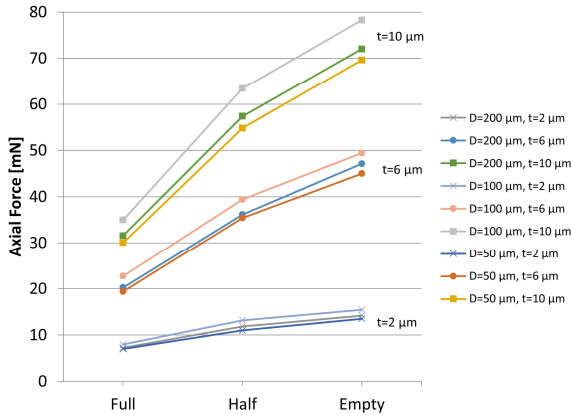


Fig. 7. Axial force variation for different modeled conditions.

The results also show that in practice where there is a considerable portion of non-full (i.e., empty and half-full) microcapsules, the elastic modulus of the composite will be lower than the neat epoxy. This interpretation from the current numerical modeling is in compliance with the previous studies of the authors [24] and shows that the modeling outputs are in compliance with the literature results.

The maximum vertical displacement in the shell was also investigated and shown in Fig. 8. The results show that the maximum vertical displacement is highly dependent upon the diameter of the microcapsules. Moreover, it can be seen that the half-full and empty conditions bring almost identical maximum vertical displacement, while comparing full and half-full conditions shows a surge from 1.46 to 1.91  $\mu\text{m}$  at diameter of 200  $\mu\text{m}$ . This is because the maximum vertical displacement occurs at the top of the microcapsules shell which has no support beneath itself both in the half-full and empty conditions. Furthermore, it can be seen that higher shell thicknesses result in lower maximum vertical displacements while this effect is almost negligible in comparison with the influence of other governing parameters.

In order to evaluate the load-deformation behavior of the composite in macro-scale, three illustrative material conditions have been selected for this macro-scale investigation, namely, neat epoxy, epoxy composites containing full and empty microcapsules with 200  $\mu\text{m}$  diameter and 2  $\mu\text{m}$ , diameter and shell thickness, respectively. The

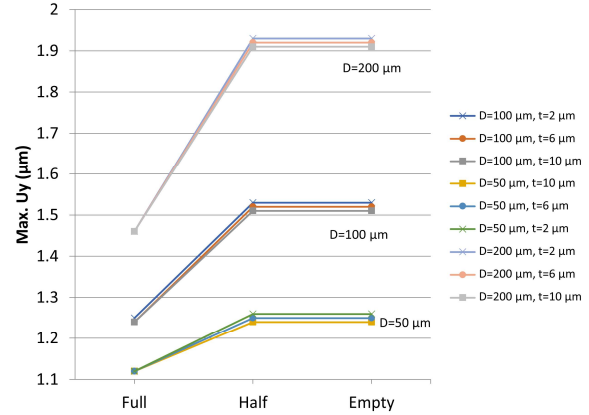


Fig. 8. Variations of the maximum vertical displacement for different modeled conditions.

elastic moduli were inserted from the extracted values in micro-scale modeling of an REV, presented in Fig. 6.

The load deformation behaviors of the samples were investigated by modeling the discussed cylindrical shaped sample subjected to a 17 MPa uniform load on the top. Figs. 9(a) to 9(c) show the horizontal deformation vectors (scaled up 100 times) for the neat epoxy, empty and full capsule conditions, respectively. A barrel-shaped form can be seen in all conditions which is generally recognized for similar compression tests with frictional jaws [44]. It can be also seen that the lateral displacement is dependent on the elastic modulus previously shown in Fig. 6.

Moreover, the vertical stress distribution shown in Fig. 9(d), revealed that except the limited zones adjacent to the end supports, the other regions experience an almost

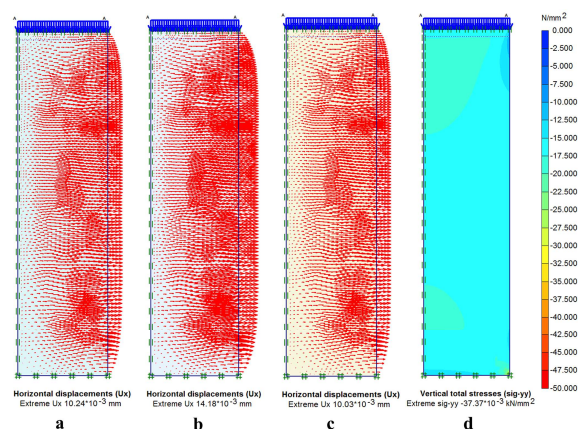


Fig. 9. Horizontal displacement vectors (100x scaled up) for: (a) neat epoxy, (b) empty microcapsule, (c) full microcapsule with 200  $\mu\text{m}$  diameter and 2  $\mu\text{m}$  diameter and shell thickness, respectively. The vertical stress distribution for (c).

constant vertical stress distribution. This shows that it was reasonable to choose a representative equivalent volume (REV) for analyzing the behavior of the material in micro-scale, as a great portion of the sample experiences an almost similar stress state. It should be noted that the stress distribution was almost identical in all three model conditions and therefore, this single illustrative figure was presented for these cases.

#### 4. Conclusion

In the current study, the load-deformation behavior of the microencapsulated-based epoxy composites was modeled in micro and macro-scales. Accepting a uniform distribution with an average spacing, a representative equivalent volume (REV) was introduced to study the composite in micro-scale. Considering different conditions of encapsulation efficiency, i.e., full, half-full and empty, varied diameter (50, 100, 200  $\mu\text{m}$ ) and thickness (2, 6, 10  $\mu\text{m}$ ) of capsules, FEM sensitivity analysis was conducted to study the influence of each governing parameter on the load-deformation behavior of the composite.

The results showed that the composite containing microcapsules with full content, exhibit slightly higher elastic modulus in comparison with the neat epoxy, while half-full and empty composites showed lower elastic modulus. Moreover, the results showed that the diameter of the capsules highly affects the overall stiffness of the composite. Indeed, the overall elastic modulus of the composite with 50  $\mu\text{m}$  microcapsules was slightly affected by the encapsulation efficiency while the composite with 200  $\mu\text{m}$  microcapsules experience more than 28% drop in its elastic modulus while going from the full to the empty capsule condition.

Furthermore, it was demonstrated that the shell thickness has a negligible effect on the overall elastic modulus of the composite. The axial force in the shell of the microcapsules was also studied which showed that the shell thickness was the most important parameter while the diameter has the least influence between the studied parameters. In addition, it was demonstrated that the emptiness of the microcapsules increases the maximum axial force in the shell.

Additionally, the vertical displacement distribution showed that the diameter and encapsulation efficiency were the most influential parameter on the maximum vertical displacement of the microcapsules. Indeed, for higher diameters of the microcapsules, higher values of maximum vertical displacement of the microcapsules were obtained. In addition, the half-full and empty conditions revealed almost the same results which were reasonable because the maximum vertical displacement of the microcapsule occurs in its crown that was unsupported both in half-full and empty conditions.

Finally, an illustrative cylindrical sample was simulated at macro-scale using the calculated elastic moduli to study the compressive behavior of the composites. The results were in compliance with the typical barrel-shaped deformation in the samples. Moreover, the results indicated that the stress distribution in the cylindrical sample was almost uniform in most zones of the sample. This confirmed that considering an equivalent volume to represent the composite (REV) was reasonable and confirms the validity of the procedure followed in this study.

#### Conflict of Interests

The authors have no conflicts of interest to declare that are relevant to the content of this article.

#### 5. References

- [1] A. Behera, *Self-Healing Materials*, In *Advanced materials*, Springer, 2022, pp. 321-358.
- [2] N.J. Kanu, E. Gupta, U.K. Vates, G.K. Singh, *Self-healing composites: A state-of-the-art review, Composites Part A: Applied Science and Manufacturing*, 121 (2019) 474-486.
- [3] T. Speck, G. Bold, T. Masselter, S. Poppinga, S. Schmier, M. Thielen, O. Speck, *Biomechanics and functional morphology of plants-Inspiration for biomimetic materials and structures*, In *Plant biomechanics*, Springer, 2018, pp. 399-433.
- [4] K.A. Althaqafi, J. Satterthwaite, N. Silikas, *A review and current state of autonomic self-healing microcapsules-based dental resin composites, Dental Materials*, 36(3) (2020) 329-342.
- [5] S.N. Gan, N. Shahabudin, *Applications of microcapsules in self-healing polymeric materials*,

- Microencapsulation-Processes, Technologies and Industrial Applications*, (2019).
- [6] J. Ren, X. Wang, D. Li, N. Han, B. Dong, F. Xing, Temperature adaptive microcapsules for self-healing cementitious materials, *Composites Part B: Engineering*, 223 (2021) 109138.
- [7] Y. Tian, M. Zheng, P. Li, J. Zhang, R. Qiao, C. Cheng, H. Xu, Preparation and characterization of self-healing microcapsules of asphalt, *Construction and Building Materials*, 263 (2020) 120174.
- [8] M. Mobaraki, M. Ghaffari, M. Mozafari, Basics of self-healing composite materials, In *Self-healing composite materials*, Woodhead Publishing Elsevier, 2020, 15-31.
- [9] M.D. Hager, P. Greil, C. Leyens, S. van der Zwaag, U.S. Schubert, Self-healing materials, *Advanced Materials*, 22(47) (2010) 5424-5430.
- [10] J.A. Syrett, C.R. Becer, D.M. Haddleton, Self-healing and self-mendable polymers, *Polymer Chemistry*, 1(7) (2010) 978-987.
- [11] M. Samadzadeh, S.H. Boura, M. Peikari, S. Kasirih, A. Ashrafi, A review on self-healing coatings based on micro/nanocapsules, *Progress in Organic Coatings*, 68(3) (2010) 159-164.
- [12] P.T. Silva, L.L.M. Fries, C.R. Menezes, A.T. Holkem, C.L. Schwan, É.F. Wigmann, J.D.O. Bastos, C.D.B. Silva, Microencapsulation: concepts, mechanisms, methods and some applications in food technology, *Ciência Rural*, 44(7) (2014) 1304-1311.
- [13] E.J. Barbero, K.J. Ford, J.A. Mayugo, Modeling self-healing of fiber-reinforced polymer-matrix composites with distributed damage, *Self-healing Materials*, Wiley, 2009.
- [14] J.D. Rule, N.R. Sottos, S.R. White, Effect of microcapsule size on the performance of self-healing polymers, *Polymer*, 48(12) (2007) 3520-3529.
- [15] S. Zwaag, Routes and mechanisms towards self healing behaviour in engineering materials, *Technical Sciences*, 58(2) (2010) 227-236.
- [16] M.M. Shokrieh, H. Rajabpour-Shirazi, M. Heidari-Rarani, M. Haghpanahi, Simulation of mode I delamination propagation in multidirectional composites with R-curve effects using VCCT method, *Computational Materials Science*, 65 (2012) 66-73.
- [17] S.D. Mookhoek, H.R. Fischer, S. van der Zwaag, A numerical study into the effects of elongated capsules on the healing efficiency of liquid-based systems, *Computational Materials Science*, 47(2) (2009) 506-511.
- [18] F.A. Gilabert, D. Garoz, W. Van Paepegem, Macro-and micro-modeling of crack propagation in encapsulation-based self-healing materials: Application of XFEM and cohesive surface techniques, *Materials & Design*, 130 (2017) 459-478.
- [19] E. Katouezadeh, S.M. Zebarjad, K. Janghorban, A practical analytic model for predicting the performance of an encapsulated polymer composite, *Applied Mathematical Modelling*, 78 (2020) 418-432.
- [20] Z. Lv, H. Chen, Analytical models for determining the dosage of capsules embedded in self-healing materials, *Computational Materials Science*, 68 (2013) 81-89.
- [21] S.V. Zemskov, H.M. Jonkers, F.J. Vermolen, Two analytical models for the probability characteristics of a crack hitting encapsulated particles: Application to self-healing materials, *Computational Materials Science*, 50(12) (2011) 3323-3333.
- [22] H.A. Algaifi, S.A. Bakar, A.R.M. Sam, A.R.Z. Abidin, S. Shahir, W.A.H. Tawayti, Numerical modeling for crack self-healing concrete by microbial calcium carbonate, *Construction and Building Materials*, 189 (2018) 816-824.
- [23] C. Xue, W. Li, J. Li, V.W. Tam, G. Ye, A review study on encapsulation-based self-healing for cementitious materials, *Structural Concrete*, 20(1) (2019) 98-212.
- [24] E. Katouezadeh, S.M. Zebarjad, K. Janghorban, Mechanical properties of epoxy composites embedded with functionalized urea-formaldehyde microcapsules containing an oxidizable oil, *Materials Chemistry and Physics*, 260 (2021) 124106.
- [25] E. Katouezadeh, S.M. Zebarjad, K. Janghorban, Investigating the effect of synthesis conditions on the formation of urea-formaldehyde microcapsules, *Journal of Materials Research and Technology*, 8(1) (2019) 541-552.
- [26] E. Katouezadeh, S.M. Zebarjad, K. Janghorban, Morphological study of surface-modified urea-formaldehyde microcapsules using 3-aminopropyltriethoxy silane, *Polymer Bulletin*, 76(3) (2019) 1317-1331.
- [27] W. K. Ding, N.P. Shah, Effect of homogenization techniques on reducing the size of microcapsules and the survival of probiotic bacteria therein, *Journal of Food Science*, 74(6) (2009) M231-M236.
- [28] S.J. Park, Y.S. Shin, J.R. Lee, Preparation and characterization of microcapsules containing lemon oil, *Journal of Colloid and Interface Science*, 241(2) (2001) 502-508.
- [29] J. Cha, J. Kim, S. Ryu, S.H. Hong, Comparison to mechanical properties of epoxy nanocomposites reinforced by functionalized carbon nanotubes and graphene nanoplatelets, *Composites Part B: Engineering*, 162 (2019) 283-288.
- [30] X. Wang, R. Han, T.L. Han, N.X. Han, F. Xing, Determination of elastic properties of urea-formaldehyde microcapsules through nanoindentation based on the contact model and the shell deformation

- theory, *Materials Chemistry and Physics*, 215 (2018) 346-354.
- [31] D. Polyzos, S.V. Tsinopoulos, D. Beskos, Static and dynamic boundary element analysis in incompressible linear elasticity, *European Journal of Mechanics-A/Solids*, 17(3) (1998) 515-536.
- [32] Y. Zhao, W. Zhang, L.P. Liao, S. Wang, W.J. Li, Self-healing coatings containing microcapsule, *Applied Surface Science*, 258(6) (2012) 1915-1918.
- [33] A. Beglarigale, D. Eyice, Y. Seki, Ç. Yalçınkaya, O. Çopuroğlu, H. Yazıcı, Sodium silicate/polyurethane microcapsules synthesized for enhancing self-healing ability of cementitious materials: Optimization of stirring speeds and evaluation of self-healing efficiency, *Journal of Building Engineering*, 39 (2021) 102279.
- [34] T. Nesterova, K. Dam-Johansen, L.T. Pedersen, S. Küil, Microcapsule-based self-healing anticorrosive coatings: Capsule size, coating formulation, and exposure testing, *Progress in Organic Coatings*, 75(4) (2012) 309-318.
- [35] H. Ullah, K. A. M Azizli, Z.B. Man, M.B.C. Ismail, M.I. Khan, The potential of microencapsulated self-healing materials for microcracks recovery in self-healing composite systems: A review, *Polymer Reviews*, 56(3) (2016) 429-485.
- [36] Y. Wang, D.T. Pham, C. Ji, Self-healing composites: A review, *Cogent Engineering*, 2(1) (2015) 1075686.
- [37] N.V.N. Jyothi, P.M. Prasanna, S.N. Sakarkar, K.S. Prabha, P.S. Ramaiah, G. Srawan, Microencapsulation techniques, factors influencing encapsulation efficiency, *Journal of Microencapsulation*, 27(3) (2010) 187-197.
- [38] M. Kosarli, D.G. Bekas, K. Tsirka, D. Baltzis, D.T. Vaimakis-Tsogkas, S. Orfanidis, G. Papavassiliou, A.S. Paipetis, Microcapsule-based self-healing materials: Healing efficiency and toughness reduction vs. capsule size, *Composites Part B: Engineering*, 171 (2019) 78-86.
- [39] A. Ahmed, K. Sanada, M. Fanni, A. Abd El-Moneim, A practical methodology for modeling and verification of self-healing microcapsules-based composites elasticity, *Composite Structures*, 184 (2018) 1092-1098.
- [40] R. De Borst, Computational methods for fracture in porous media: Isogeometric and extended finite element methods, Elsevier, 2017.
- [41] A. F. Bower, Applied mechanics of solids, CRC Press 2009.
- [42] N. Khun, D. Sun, M. Huang, J. Yang, C.J. Yue, Wear resistant epoxy composites with diisocyanate-based self-healing functionality, *Wear*, 313(1-2) (2014) 19-28.
- [43] M. Samadzadeh, S.H. Boura, M. Peikari, A. Ashrafi, M. Kasirha, Tung oil: An autonomous repairing agent for self-healing epoxy coatings, *Progress in Organic Coatings*, 70(4) (2011) 383-387.
- [44] J.D. Littell, C.R. Ruggeri, R.K. Goldberg, G.D. Roberts, W.A. Arnold, W.K.E. Binienda, Measurement of epoxy resin tension, compression, and shear stress-strain curves over a wide range of strain rates using small test specimens, *Journal of Aerospace Engineering*, 21(3) (2008) 162-173.